

# <sup>31</sup>P Knight shifts and spin dynamics in Si:P at temperatures comparable to the Fermi temperature

M. J. R. Hoch

*School of Physics, University of the Witwatersrand, Johannesburg 2050, South Africa  
and National High Magnetic Field Laboratory, Tallahassee, Florida 32310, USA*

D. F. Holcomb

*Laboratory of Atomic and Solid State Physics, Cornell University, Ithaca, New York 14853, USA*

(Received 13 May 2004; revised manuscript received 27 September 2004; published 26 January 2005)

Meintjes, Danielson, and Warren (MDW) have recently reported the results of high-temperature NMR and Hall effect experiments using samples of Si:P with P concentrations at, and above, the metal-insulator transition value of  $3.7 \times 10^{18} \text{ cm}^{-3}$ . MDW interpret their measurements of the <sup>31</sup>P Knight shift ( $K$ ) and relaxation rate ( $1/T_1$ ) in terms of a model that emphasizes the role of impurity bands for just-metallic samples. We show that a number of features of the MDW data can be usefully explored by use of a less elaborate approach. An extension of the Korringa relation, which relates  $K$  and  $1/T_1$ , into regimes where  $k_B T$  is comparable to, or greater than, the Fermi energy  $E_F$  confirms that the electron-nucleus hyperfine interaction does, indeed, control Knight shift and relaxation rate in this high- $T$  regime. We also explore insights gained by comparison of the MDW data with the extensive earlier NMR data at 4.2 K and below. The extended Korringa relation provides a method for analyzing high- $T$  NMR data in other low carrier density systems.

DOI: 10.1103/PhysRevB.71.035115

PACS number(s): 71.23.-k, 71.55.Cn, 76.60.Cq, 76.60.Es

## INTRODUCTION

The metal-insulator (MI) transition in heavily doped semiconductors, especially Si:P, has been the subject of intensive investigation for several decades.<sup>1-3</sup> Much of the experimental work has been carried out at temperatures at and below 4 K because of interest in exploring the possible quantum critical character of the transition. A detailed description of the electronic structure for samples with impurity concentration just above that of the MI transition remains elusive. Much of the elusiveness stems from smudging effects caused by the statistically inhomogeneous impurity atom distribution. Meintjes, Danielson, and Warren<sup>4</sup> (MDW) have recently presented <sup>29</sup>Si and <sup>31</sup>P Knight shift ( $K$ ) and NMR relaxation time ( $T_1$ ) data for a number of Si:P samples, with P concentration ranging from  $n_p \approx n_c$  to  $n_p = 20n_c$ . Their data, taken in the 100 to 500 K temperature range, significantly extend earlier NMR data on this system obtained at low temperatures.<sup>5-8</sup> In degenerate metallic systems the nuclear spin-lattice relaxation rate is proportional to  $T$ . The MDW <sup>31</sup>P data show increasing departures from conventional metallic behavior as the doping level decreases towards  $n_c$ . They have analyzed the results in terms of a model that probes the effects of impurity-derived energy bands well separated from the Si host conduction band. Exploration of the model is based on numerical integration of the effects of thermal excitation from the lowest impurity band to upper impurity bands and the Si conduction band. The MDW model is productive, particularly in interpreting the unusual temperature dependence of the <sup>31</sup>P  $T_1$  data for samples with values of  $n_p$  just above the MI transition.

The general conclusions drawn from the MDW interpretation of the NMR data are consistent with the picture developed in the far-IR reflectance study by Gayman, Geserich, and von Löhneysen<sup>9</sup> (GGL). This far-IR work provided one

of the first clean experimental studies of the long-invoked but seldom-measured impurity bands.

It is important to note that, while valuable information about the energy level structure, and electron occupation thereof, can be drawn from NMR data, these data do not typically provide much information about the evolution of the electron transport properties in this barely metallic system. This assessment also applies to the MDW work.

The MDW model introduces an impurity energy band formed from the valley-orbit split ground state of the isolated impurity, with  $s$ -function symmetry around the donor core, as well as two impurity bands at higher energies formed from the excited  $p$ -symmetry states of the isolated impurity (see Fig. 10 of Ref. 4). For samples with  $n_p > 10^{19} \text{ cm}^{-3}$ , it seems likely to us that the assumed integrity of these upper bands, and a categorization of states on the basis of the symmetry of wave functions of the isolated donor, is no longer valid. This conclusion is suggested both by the existence of strong screening of the  $P$ -donor potential by delocalized electrons at these higher impurity concentrations, and by the optical studies of GGL which show no evidence of transitions ascribable to such bands. In their treatment MDW do allow for merging of the impurity bands with the conduction band as the donor concentration increases.

As an alternative to the numerical approach involving impurity bands adopted by MDW, we decided to approach the MDW data from the high concentration end using models appropriate to the metallic state. For metals, the Korringa relation<sup>10,11</sup> connects  $K$ ,  $T_1$ , and the absolute temperature  $T$ . We introduce an extension of the Korringa relation into temperature ranges where  $k_B T$  approaches, or exceeds, the Fermi energy  $E_F$ . The Si:P samples with low Fermi temperatures offer an opportunity for examining the evolution of spin susceptibility and NMR properties as one moves from the condition  $T/T_F < 1$  to  $T/T_F > 1$ .

TABLE I. MDW Si:P sample parameters.

Sample	$n/n_c$	$T_F$ (K)	$K_{pk}$ (100 K) ppm	$\chi_s$ [QM (Ref. 14)] (77 K) $10^{-8}$ emu $\text{cm}^{-3}$	$P_f$ (100 K) $10^{24}$ $\text{cm}^{-3}$	$P_f$ (4.2 K) $10^{24}$ $\text{cm}^{-3}$	MDW $P_f$ $10^{24}$ $\text{cm}^{-3}$
80	21.4	730	2450	8.9	0.26	0.26 (Ref. 6) (from $\langle K \rangle$ )	0.24
10	2.7	180	3900	3.8	0.16 <sup>a</sup>	$\approx 0.22$ (Ref. 6)	
7	1.9	142	4050	2.9	0.12 <sup>a</sup>		
4	1.07	98	5000 (est)	2.1	0.11 <sup>a</sup>		0.33 (s-band only)

<sup>a</sup>Denotes that  $\chi_s$  values at 100 K were obtained by extrapolation using data from Ref. 14.

It should be noted that in the statistically inhomogeneous Si:P samples, we expect there to be a spatial distribution of values of the local  $e$ - $n$  hyperfine coupling constant and of the  $^{31}\text{P}$  NMR parameters  $K$  and  $T_1$ . The effects of this distribution are particularly evident in samples at high impurity concentration, where the NMR absorption line is broad and asymmetric.<sup>5-8</sup> The value of  $T_1$  is similarly a function of the frequency of the RF excitation.<sup>12,13</sup> For the lower concentration samples of MDW (samples 4, 7, and 10), Fig. 2 in Ref. 4 shows the distribution of values of  $K$  to be significantly narrowed. One would then expect a matching uniformity of values of  $T_1$  for the full  $^{31}\text{P}$  spin system.

Thus, while in this paper we will refer to *values* of  $K$  and  $T_1$ , it should be recognized that there is typically a distribution of values of both quantities over the NMR absorption line. The distribution is most pronounced for sample 80.

### SAMPLE PARAMETERS

Table I collects various experimental data and calculated values of relevant physical parameters for the samples used by MDW in their experiments.

For samples of Si:P with  $n_p \gg n_c$ , we calculate values of  $T_F$  using the expression  $T_F = (3\pi^2 n/l)^{2/3} \hbar^2 / 2k_B m^*$ , with the density of states effective mass  $m^* = 0.33 m_e$  and the degeneracy factor  $l=6$  to allow for the sixfold degeneracy of the bottom of the conduction band. If we apply this calculation to the MDW samples, values of  $T_F$  are as given. Calculation of values of  $T_F$  in this fashion gives values progressively more questionable as we move from sample 80, with most carriers in the conduction band, to sample 4 where the applicability of the parabolic band model is open to question. We return later to comments on this point.

The Knight shift for a metal may be written in a standard form<sup>10</sup> as

$$K = \frac{8\pi}{3} \sum_k |u_k(0)|^2 \chi_k, \quad (1)$$

where  $|u_k(0)|^2$  is the probability density at the nucleus for carriers of wave-vector  $k$ , with normalization such that

$\int |u_k(0)|^2 dV = 1$ , and  $\chi_k$  is the spin susceptibility contribution from these carriers. Assuming that the probability density is not strongly  $k$ -dependent and that the system is homogeneous, converting the sum to an integral gives

$$K = \frac{8\pi}{3} \left( \frac{P_f}{n} \right) \chi_s, \quad (2)$$

where  $\chi_s = \int \chi(\epsilon) \rho(\epsilon) d\epsilon$  and setting  $P_f = n |u_k(0)|^2$  defines  $P_f$ .

We have noted that in a statistically inhomogeneous, low density metal such as Si:P, we expect the value of  $P_f$  to vary from site to site. The local susceptibility  $\chi_s$  could also vary from site to site, as it dramatically does at low temperatures in samples with  $n_p$  near  $n_c$ .<sup>6</sup> We proceed under the assumption that this low temperature magnetic inhomogeneity, which may be occasioned by bottlenecks in electron spin relaxation, is washed out by thermal stirring at 77 K and above. This assumption is supported by the spin susceptibility studies.<sup>14,15</sup>

Combining the MDW data for  $K_{pk}$  (their Fig. 3) with the experimental spin susceptibility data<sup>14</sup> permits one to use Eq. (2) to extract values of  $P_f$ , a measure of the average electronic probability density at the  $^{31}\text{P}$  nucleus (sixth column of Table I). These values then permit useful comparisons with both the MDW values for  $P_f$  (which are used as fitting parameters in their approach) and the values at low temperature.<sup>5-7</sup>

We note that the two values of  $P_f$  for sample 80 from our analysis and from the MDW paper are in full agreement, a satisfying checkpoint. The drift downward in values of  $P_f$  in Column 6 for samples with lower concentration is qualitatively consistent with the low-temperature analysis of Alloul and Dellowe.<sup>6</sup>

Secondly, we note from Table I that there is a downward trend in the  $P_f$  values at 100 K with decreasing  $n/n_c$ . For sample 4, the fitted value of 0.33 from MDW provides support for their numerical model. It suggests that the low value of 0.11 from direct use of Eq. (2) stems from failure to recognize the shift in the nature of the impurity band wave functions from predominantly  $s$  type to substantially  $p$  type as the temperature rises. However, for samples with electron concentration near the value  $n_c$ , one would expect to see a

similar recovery of values of  $P_f$  in the low-temperature data of Alloul and Dellouve,<sup>6</sup> where one would expect full occupation of the  $s$ -type impurity band. This recovery is not observed. We conclude that the full story of the evolution of values of  $P_f$  remains unresolved.

### MODIFICATIONS OF STANDARD NMR THEORETICAL EXPRESSIONS

In the temperature range of the MDW experiments, for the low-electron density, just-metallic Si:P samples, the usual metallic condition  $k_B T \ll E_F$  does not hold. It is therefore necessary to use modified expressions for  $K$  and  $T_1$ . At temperatures below the Fermi temperature  $T_F$ , the density of states function may be expanded about the  $T=0$  chemical potential,  $\mu_o=E_F$ , in powers of  $(k_B T/E_F)^2$  in the usual way.<sup>16,17</sup> The expression for the susceptibility becomes

$$\chi_s = \left( \frac{\gamma_s^2 \hbar^2}{2} \right) \rho(\mu) \left[ 1 + \frac{\pi^2}{6} \left( \frac{d^2 \ln \rho(\epsilon)}{d\epsilon^2} \right)_{\mu} k_B^2 T^2 + \dots \right], \quad (3)$$

where  $\gamma_s$  is the electron magnetogyric ratio.

For the special case of a noninteracting gas of independent electrons

$$\rho(\epsilon) = \left( \frac{3n}{4\epsilon_F^{3/2}} \right) \epsilon^{1/2} \quad (4)$$

and, for  $T < T_F$ , Eq. (2) may be written

$$K = 2\pi \left( \frac{\gamma_s^2 \hbar^2}{2} \right) \frac{P_f}{k_B T_F} \left[ 1 - \frac{\pi^2}{12} \left( \frac{T}{T_F} \right)^2 \right], \quad (5)$$

with higher order terms in the expansion omitted. Similarly, for  $T > T_F$ , we obtain

$$K = \frac{8\pi}{3} \left( \frac{\gamma_s^2 \hbar^2}{2} \right) \frac{P_f}{k_B T} \left[ 1 - \frac{2\sqrt{2}\pi}{3} \left( \frac{T_F}{T} \right)^{3/2} \right], \quad (6)$$

where again higher order terms have been omitted. While not explicitly denoted, we allow that the value of  $P_f$  may carry a temperature dependence, as mentioned above.

The appearance of a temperature dependence in  $K$  signals the change from Pauli susceptibility (for  $T \ll T_F$ ) to the high-temperature Curie law form ( $T \gg T_F$ ). Using numerical integration, the complete expressions for  $\chi_s$  can be evaluated over the entire temperature range. MDW have used such a numerical approach in their analysis.

Expressions for  $1/T_1$  at temperatures such that  $k_B T \ll E_F$  or  $k_B T \gg E_F$  are given below. Using a fixed value of probability density  $P_f$  and assuming isotropic properties in  $k$  space similar to those used in the Knight shift case, we have

$$\frac{1}{T_1} = \frac{64}{9} \pi^3 \hbar^3 \gamma_s^2 \gamma_I^2 \left( \frac{P_f}{n} \right)^2 k_B T \int_0^\infty \rho^2(\epsilon) \left( \frac{df}{d\epsilon} \right)_\mu d\epsilon, \quad (7)$$

where  $f$  is the Fermi function and  $\gamma_I$  the nuclear magnetogyric ratio. Expanding  $\rho^2(\epsilon)$  about  $\mu$  and integrating gives

$$\frac{1}{T_1} = \frac{64}{9} \pi^3 \hbar^3 \gamma_s^2 \gamma_I^2 \left( \frac{P_f}{n} \right)^2 k_B T \rho^2(\mu) \left[ 1 + \frac{\pi^2}{6} \frac{(k_B T)^2}{\rho^2(\mu)} \left( \frac{d^2 \rho}{d\epsilon^2} \right)_\mu \right]. \quad (8)$$

For the independent electron case, for  $T < T_F$ , this expression becomes

$$\frac{1}{T_1} = 4\pi^3 \hbar^3 \gamma_s^2 \gamma_I^2 P_f^2 \frac{1}{k_B T_F} \left( \frac{T}{T_F} \right) \left[ 1 - \frac{\pi^2}{12} \left( \frac{T}{T_F} \right)^2 \right]. \quad (9)$$

Similarly, for  $T > T_F$ , we obtain

$$\frac{1}{T_1} = \frac{64}{3\sqrt{\pi}} \pi^3 \hbar^3 \gamma_s^2 \gamma_I^2 P_f^2 \frac{1}{k_B T_F} \left( \frac{T}{T_F} \right)^{1/2} \times \left[ 1 - \sqrt{\frac{2}{\pi}} \left( \frac{\sqrt{2}-1}{3} \right) \left( \frac{T_F}{T} \right)^{3/2} \right]. \quad (10)$$

Higher order terms in  $T/T_F$  and  $T_F/T$  are omitted in Eqs. (9) and (10), respectively.

The  $T^{1/2}$  dependence of  $1/T_1$  in the high  $T$  limit is consistent with an expression given for relaxation in semiconductors by Abragam.<sup>11</sup> Note that the exponent value 1/2 is determined by the form of the energy dependence in the density of states function which for an independent electron gas is  $\rho(\epsilon) \propto \epsilon^{1/2}$ , as given in Eq. (4). This  $T^{1/2}$  dependence is not observed by MDW for either the <sup>31</sup>P or <sup>29</sup>Si spin systems.

*Modified Korringa relationship for  $T$  comparable to  $T_F$ .* We have found it useful to use the expressions for  $K$  and  $1/T_1$  in Eqs. (5), (6), (9), and (10) to form temperature-dependent Korringa products  $K^2 T_1 T$ . If the electron-nucleus hyperfine coupling controls both Knight shift and relaxation rate, the Korringa product does not depend upon the specific value of  $P_f$ .

Using Eqs. (5) and (9) gives the Korringa product  $\kappa$  for temperatures  $T < T_F$

$$\kappa = K^2 T_1 T = \frac{\hbar \gamma_s^2}{4\pi k_B \gamma_I^2} F \left( \frac{T}{T_F} \right), \quad (11)$$

with  $F(T/T_F) = [1 - (\pi^2/12)(T/T_F)^2]$ , a factor which tends to unity for  $T/T_F \ll 1$ .

Similarly, for  $T > T_F$  Eqs. (6) and (10) give

$$\kappa = K^2 T_1 T = \frac{\hbar \gamma_s^2}{4\pi k_B \gamma_I^2} \left( \frac{\sqrt{\pi}}{3} \right) G \left( \frac{T}{T_F} \right), \quad (12)$$

with

$$G \left( \frac{T}{T_F} \right) = \left( \frac{T_F}{T} \right)^{3/2} \frac{\left[ 1 - \frac{2\sqrt{2}\pi}{3} \left( \frac{T_F}{T} \right)^{3/2} \right]^2}{\left[ 1 - \frac{\sqrt{2}\sqrt{2}-1}{\pi} \left( \frac{T_F}{T} \right)^3 \right]}.$$

The factor  $G(T/T_F)$  retains a temperature dependence for all  $T/T_F$ .

The quantity  $(\hbar \gamma_s^2 / 4\pi k_B \gamma_I^2) = 1.61 \times 10^{-6}$  s K for free electrons ( $g=2$ ) is the usual Korringa constant applicable to simple metals at low temperatures. For metals with low carrier densities, such as doped semiconductors,  $T_F$  will be low

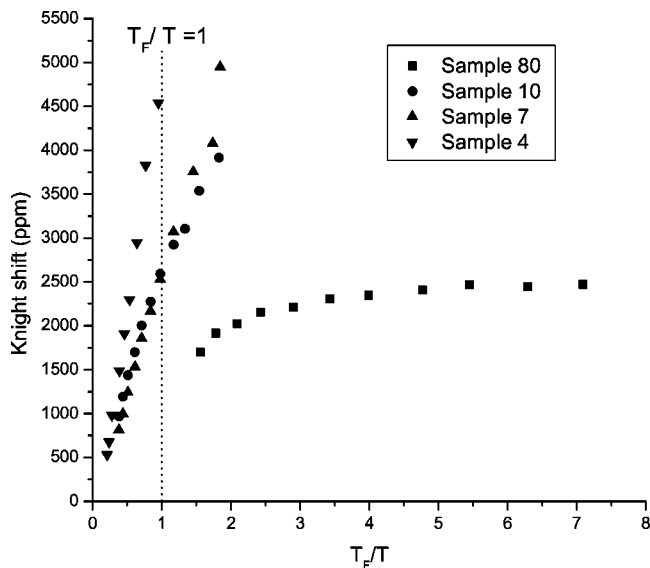


FIG. 1.  $^{31}\text{P}$  Knight shifts as a function of the reduced reciprocal temperature  $T_F/T$  for Si:P samples 80, 10, 7, and  $4(\times 10^{18} \text{ cm}^{-3})$ . Experimental data for  $K$  and  $T_1$  were provided by Meintjes and Warren (Ref. 4).

and the correction factors to the Korringa product given in Eqs. (11) and (12) become important.

#### APPLICATION OF THE KORRINGA RELATION APPROACH

Figure 1 displays the  $^{31}\text{K}$  data from Ref. 4, plotted versus  $T_F/T$ , with  $T_F$  values taken from Table I. We note that for sample 4, for which  $T_F/T < 1$  over the full measurement range, the temperature dependence of  $K$  is very close to  $1/T$ , giving support to the basic Knight shift relationship in Eq. (1). The measurements of  $\chi_s$  by Quirt and Marko<sup>14</sup> show a similar Curie-like  $1/T$  dependence at high temperatures. The  $^{31}\text{K}$  values for samples 10 and 7, for which  $T_F/T$  passes through 1.0, show Curie-like (or Curie-Weiss-like) behavior as  $T$  increases.

This behavior is consistent with the change from Fermi-Dirac to Boltzmann statistics for the electron system at high temperatures. The temperature dependence of  $^{31}\text{K}$  found for sample 80 shows a departure from conventional metallic behavior where  $K$  is independent of  $T$ . This departure signals the rise of  $T$  towards  $T_F$  at the highest  $T$  values. The Knight shift behavior with  $T_F/T$  for samples 10 and 7 is seen to be intermediate between that of samples 80 and 4.

In Fig. 2 the  $^{31}\text{P}$  Knight shift data for sample 80 is plotted as a function of  $T$  together with adjusted values  $^{31}\text{K}_{\text{adj}}$  which are obtained by dividing the measured  $^{31}\text{K}$  values by the factor  $F(T/T_F)$ . This factor is introduced in Eq. (5) and defined following Eq. (11). This adjustment process is found to compensate for the decrease of  $^{31}\text{K}$  with rising  $T$ , giving a constant value for  $^{31}\text{K}_{\text{adj}}$  within experimental uncertainty.

We now examine the  $T$  dependence of the Korringa product  $\kappa = K^2 T_1 T$ . Figure 3(b) shows values of this product, based on the data of MDW, as a function of temperature for

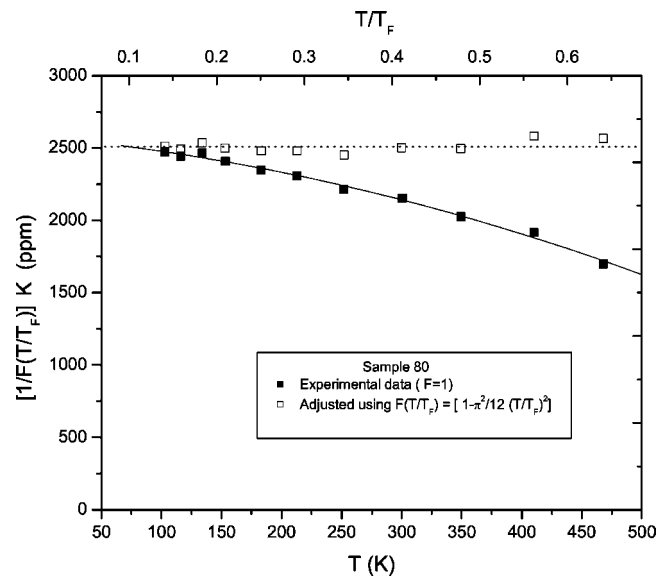


FIG. 2.  $^{31}\text{P}$  Knight shifts versus  $T$  for sample 80. Both unadjusted  $^{31}\text{K}$  (closed symbols) and adjusted  $^{31}\text{K}_{\text{adj}} = ^{31}\text{K}/F(T/T_F)$  data values (open symbols) are shown. The factor  $F(T/T_F)$  is defined following Eq. (11) in the text. The curves are to aid the eye. The full curve is a polynomial fit to the MDW (Ref. 4) data and the dashed curve gives the average of the adjusted Knight shift values  $^{31}\text{K}_{\text{adj}}$  for  $T < 175$  K.

sample 80. (Experimental values for  $K$  and  $T_1$  are those given by MDW in Ref. 4. MDW show estimated uncertainties in their values but we have chosen not to give uncertainties in the values of  $\kappa$  plotted in Figs. 3, 4, and 5. The degree of departure of data points from a smooth curve gives a measure of the experimental uncertainty.) There is a marked temperature dependence. In Fig. 3(a), this temperature dependence is eliminated by using the factor  $1/F(T/T_F)$  to adjust the product values, giving  $\kappa_{\text{adj}}$ . The theoretical single electron value of  $\kappa$  for the  $^{31}\text{P}$  system of  $1.61 \times 10^{-6}$  s K is indicated. The  $T/T_F$  adjusted Korringa products  $\kappa_{\text{adj}}$  for sample 80 have an average value of  $1.0 \times 10^{-6}$  s K, which is significantly lower than the theoretically predicted value for  $T < T_F$ .

In the present analysis, the Knight shift  $K$  is represented by values of  $K_{pk}$ , which are derived from the frequency position of the peak amplitude of the  $^{31}\text{P}$  resonance lines. (These values are taken from Ref. 4.) For sample 80, and to a lesser degree for samples 10 and 7, the observed NMR absorption line is noticeably asymmetric. One can argue that it would be better to use  $\langle K \rangle$ , the value of  $K$  at the mean frequency of the absorption line. Previous low-temperature determinations<sup>7</sup> suggest that  $\langle K \rangle$  is larger than  $K_{pk}$  by roughly 10 to 15% for sample 80. Thus, using  $\langle K \rangle$  might increase the derived value of  $K^2 T_1 T$  to about  $1.2 \times 10^{-6}$  s K. In this low-density, positionally disordered system, this discrepancy from the  $1.61 \times 10^{-6}$  s K value could arise from a variety of sources, which we do not pursue further herein.

A comparison of the present plots obtained for sample 80 with the plots for this sample given by MDW (Figs. 8 and 9 of Ref. 4) provides a cross check between our analysis and

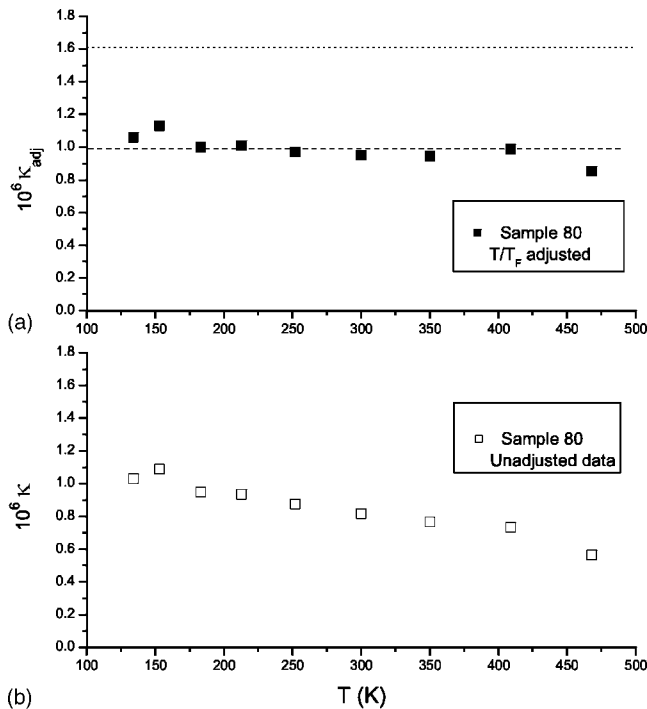


FIG. 3. <sup>31</sup>P Korrington products  $\kappa=K^2T_1T$  versus  $T$  for sample 80. The plot in (b) gives the unadjusted values, based on the MDW (Ref. 4) data, while (a) shows adjusted data values  $\kappa_{\text{adj}}=^{31}K/F(T/T_F)$  using the factor  $F(T/T_F)$ , defined following Eq. (11), which compensates for the finite  $T/T_F$  ratio. The dotted line in Fig. 3(a) shows the theoretically predicted value for the Korrington product in the metallic parabolic band model for  $T \ll T_F$  ( $1.61 \times 10^{-6}$  s K) while the dashed line shows the average value of  $\kappa_{\text{adj}}$ .

that of MDW. The two approaches are found to give consistent descriptions, as might be expected for this most metallic sample. Table I shows the present value of  $P_f$  for sample 80, in comparison with the value obtained by MDW.

All data for sample 80 lie in the  $T < T_F$  regime. For samples 4, 7, and 10, the data fall in a temperature range such that  $T \geq T_F$ , with  $T_F < 200$  K for all three concentrations. But the stronger condition  $T \gg T_F$  is not reached in the MDW measurements for samples 7 and 10, and is only approached for sample 4 at the highest temperatures used. However, since the higher order correction terms for the relevant Eqs. (6) and (10) have not been obtained, we investigate the application of the high-temperature, modified Korrington relation given in Eq. (12) to all three of the lower concentration samples with the expectation that agreement between theory and experiment will improve as  $T/T_F$  increases.

Figure 4(b) shows a plot of the Korrington product  $\kappa=K^2T_1T$  versus  $T$  for samples 7 and 10, while Fig. 4(a) shows adjusted values  $\kappa_{\text{adj}}=K^2T_1T/(T_F/T)^{3/2}$ , for these samples. The plotted points are for temperatures such that the condition  $T_F/T < 1$  is always satisfied. At high temperatures, the adjusted values  $\kappa_{\text{adj}}$  approach the high-temperature theoretically predicted value of  $0.95 \times 10^{-6}$  s K for a parabolic band. This value is shown as the dashed line in Fig. 4(a). Use of the high- $T$  asymptotic limit factor  $(T_F/T)^{3/2}$  rather than the

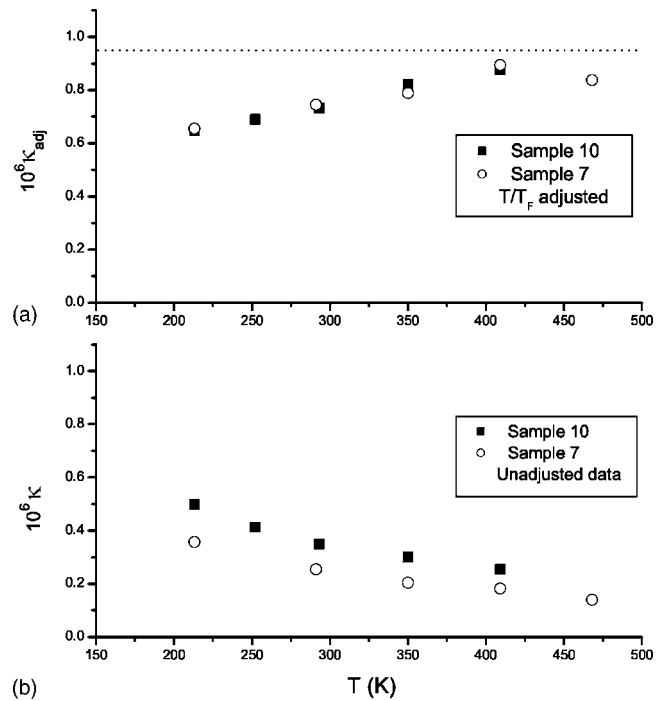


FIG. 4. <sup>31</sup>P Korrington products  $\kappa=K^2T_1T$  versus  $T$ , for samples 7 and 10, at temperatures  $T > T_F$  for both. The plot in (b) gives the unadjusted values, based on the MDW data (Ref. 4), while (a) shows adjusted values  $\kappa_{\text{adj}}=\kappa/[(T/T_F)^{3/2}]$  using the factor  $[(T/T_F)^{3/2}]$ , taken from Eq. (12) in the high- $T$  limit. The dotted line in Fig. 3(a) shows the theoretically predicted high- $T$  asymptotic ( $T \gg T_F$ ) value for the modified Korrington product  $K^2T_1T/G(T/T_F) = K^2T_1T/[(T/T_F)^{3/2}] = \hbar \gamma_s^2 / 4\pi k_B \gamma_I^2$ , in the parabolic band model ( $0.95 \times 10^{-6}$  s K).

expansion expression  $1/G(T_F/T)$  is preferred here because, for these two samples, the condition  $T \gg T_F$  is not realized. This means that higher order terms than those given in the expansion in Eq. (12) would be needed to avoid overcorrecting by the adjustment factor. Use of  $(T_F/T)^{3/2}$  leads to under correction as may be seen in Fig. 4(a). Nevertheless, the trend towards the theoretically predicted value of  $\kappa$  with increasing  $T$  is clear.

Figure 5 shows  $\kappa=K^2T_1T$  versus  $T$  for sample 4 together with adjusted values  $K^2T_1T/(T_F/T)^{3/2}$  and  $K^2T_1T/G(T_F/T)$ . The overcorrection effect, mentioned above, is clearly demonstrated when the correction factor  $1/G(T_F/T)$  [defined following Eq. (12)] is used rather than the factor  $1/(T_F/T)^{3/2}$ . We note that the two sets of values converge as  $T/T_F$  increases, as they should. The scatter in this plot is more pronounced than in the plots for the higher dopant concentrations. This scatter reflects the great difficulty of making the experimental NMR measurements at high temperatures in this sample with low <sup>31</sup>P concentration. Achievement of acceptable values of signal-to-noise for this sample at high temperatures by MDW is impressive.

Examination of Figs. 4 and 5 shows that at temperatures exceeding the Fermi temperature, the high- $T$  Korrington-type relation, given in Eq. (12), provides a useful basis for interpreting the NMR results obtained by MDW for just-metallic Si:P samples. Our analysis shows that that the Knight shift

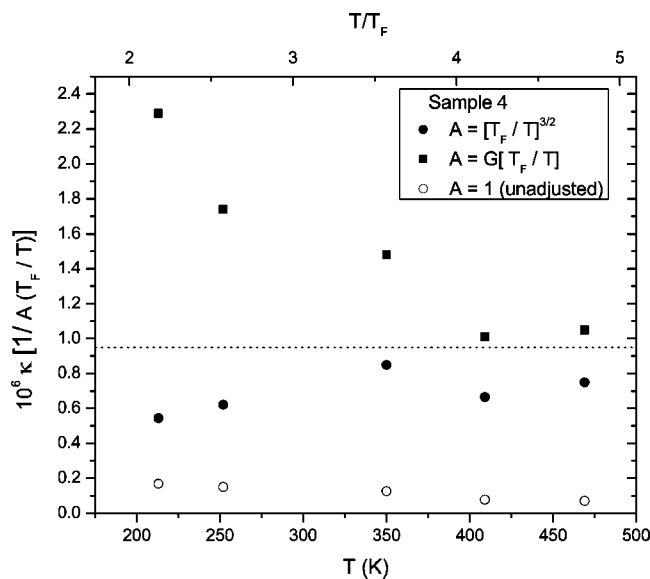


FIG. 5.  $^{31}\text{P}$  Korringa product  $\kappa = K^2 T_1 T$  versus  $T$ , for sample 4, at temperatures  $T > T_F$ . The values are plotted in three ways. The open circles give the unadjusted MDW (Ref. 4) products, the solid squares the adjusted values  $\kappa_{\text{adj}} = K^2 T_1 T / G(T/T_F)$ , with  $G(T/T_F)$  defined following Eq. (12), and the solid circles the adjusted Korringa values using  $G(T/T_F) \approx (T/T_F)^{3/2}$  corresponding to the high- $T$  approximation. The dotted line shows the theoretically predicted value for the modified Korringa product  $K^2 T_1 T / [(T/T_F)^{3/2}]$  in the parabolic band model for  $T \gg T_F$  ( $0.95 \times 10^{-6}$  s K).

and spin-lattice relaxation mechanisms are accounted for in a metallic description of this system, for all  $n > n_c$ , provided allowance is made for the change in electron statistics from Fermi to Boltzmann. An advantage of the present analysis, using the generalized Korringa product expressions close to the MI transition, is that effects of uncertainties in the values of the probability density factor  $P_f$  with temperature are avoided.

## CONCLUSIONS

For samples of heavily doped Si with impurity concentrations just above  $n_c$ , such as sample 4, the MDW interpreta-

tion of their high-temperature NMR results gives strong support to the proposition that a separated energy band of impurity-derived levels exists. As the concentration rises towards that of sample 80, with phosphorus concentration  $n_p \approx 20n_c$ , the impurity bands merge with the conduction band to form a conventional, but disordered, metallic material. Indeed, the need for the impurity band model becomes less clear for higher concentrations, near and above  $3n_c$ .

We have approached analysis of the high-temperature data of MDW by introducing temperature-dependent corrections to the Korringa formulation often used to analyze NMR properties of metals. These corrections allow for the fact that the usual assumption for metals, that  $T \ll T_F$ , does not apply to just-metallic semiconductors. Our development and application of appropriate temperature-dependent modifications of the Korringa relation confirm the implicit assumption of MDW that the Knight shift and relaxation rate ( $K$  and  $T_1$ ) are controlled by the  $\mathbf{I} \cdot \mathbf{S}$  electron-nucleus interaction in all four of the MDW samples, even when one sees the unusual *reverse* temperature-dependence of the  $^{31}\text{P}$  relaxation rate shown in Fig. 4 of MDW.

Our approach, which involves modification of conventional Korringa analysis to allow for the low Fermi temperatures that occur in heavily doped semiconductors, sidesteps the uncertainties in the behavior of the hyperfine coupling constant as a function of concentration and temperature. The modified Korringa relations which we introduce should be applicable to other low electron density metallic systems when NMR measurements are made at temperatures comparable to the Fermi temperature.

## ACKNOWLEDGMENTS

Many discussions and correspondence with W.W. Warren and Ernesta Meintjes are gratefully acknowledged. In particular, at various stages of our interactions, they have generously shared data and explanations of their pathway. Financial support for one of us (M.J.R.H.) was provided by the South African National Science Foundation and the University of the Witwatersrand, Johannesburg.

<sup>1</sup>M. P. Sarachik, in *Metal-Insulator Transitions Revisited*, edited by P. P. Edwards and C. N. R. Rao (Taylor and Francis, London, 1995), pp. 79–103.  
<sup>2</sup>D. Belitz and T. R. Kirkpatrick, *Rev. Mod. Phys.* **66**, 261 (1994).  
<sup>3</sup>P. P. Edwards, R. L. Johnston, F. Hensel, C. N. R. Rao, and D. P. Tunstall, in *Solid State Physics*, edited by H. Ehrenreich and F. Spaepen (Academic Press, New York, 1999), Vol. 52.  
<sup>4</sup>E. M. Meintjes, R. Danielson, and W. W. Warren, Jr., *Phys. Rev. B* **71**, 035114 (2005); E. M. Meintjes, Ph.D. thesis, Oregon State University, 1998, available from UMI Microfilms, Ann Arbor, MI.  
<sup>5</sup>R. K. Sundfors and D. F. Holcomb, *Phys. Rev.* **136**, A810 (1964).  
<sup>6</sup>H. Alloul and P. Dellouve, *J. Phys. (Paris), Colloq.* **49**, 1185 (1988); *Phys. Rev. Lett.* **59**, 578 (1987).  
<sup>7</sup>G. C. Brown and D. F. Holcomb, *Phys. Rev. B* **10**, 3394 (1974).  
<sup>8</sup>Seiichiro Ikehata, Wataru Sasaki, and Shun-ichi Kobayashi, *J.*

*Phys. Soc. Jpn.* **39**, 1492 (1975).

<sup>9</sup>A. Gaymann, H. P. Geserich, and H. v. Löhneysen, *Phys. Rev. B* **52**, 16 486 (1995).

<sup>10</sup>C. P. Slichter, *Principles of Magnetic Resonance*, 3rd ed. (Springer, Berlin, 1996).

<sup>11</sup>A. Abragam, *The Principles of Nuclear Magnetism* (Oxford University Press, Oxford, 1961).

<sup>12</sup>S. Kobayashi, Y. Fukagawa, S. Ikehata, and W. Sasaki, *J. Phys. Soc. Jpn.* **45**, 1276 (1978).

<sup>13</sup>M. J. Hirsch and D. F. Holcomb, *Phys. Rev. B* **33**, 2520 (1986).

<sup>14</sup>J. D. Quirt and J. R. Marko, *Phys. Rev. B* **7**, 3842 (1973).

<sup>15</sup>A. Roy and M. P. Sarachik, *Phys. Rev. B* **37**, 5531 (1998).

<sup>16</sup>N. F. Mott and H. Jones, *Theory of the Properties of Metals and Alloys* (Clarendon Press, Oxford, 1936).

<sup>17</sup>E. Kiess, *Am. J. Phys.* **55**, 1006 (1987).